



Enhanced mineralization of pharmaceuticals by surface oxidation over mesoporous γ -Ti-Al₂O₃ suspension with ozone

Jishuai Bing^{a,b}, Chun Hu^{a,b,*}, Lili Zhang^a

^a Key Laboratory of Drinking Water Science and Technology, Research Center for Eco-Environmental Sciences, Chinese Academy of Sciences, Beijing 100085, China

^b University of Chinese Academy of Sciences, Beijing 100049, China

ARTICLE INFO

Article history:

Received 15 April 2016

Received in revised form 4 September 2016

Accepted 6 September 2016

Available online 9 September 2016

Keywords:

γ -Ti-Al₂O₃

Catalytic ozonation

Pharmaceuticals

Reactive oxygen species

ABSTRACT

Titanium-doped mesoporous γ -Al₂O₃ (γ -Ti-Al₂O₃) was prepared by an evaporation-induced self-assembly method and characterized by X-ray diffraction, X-ray photoelectron spectroscopy, nitrogen adsorption-desorption, scanning electron microscope, and FTIR spectra of chemisorbed pyridine. γ -Ti-Al₂O₃ revealed excellent catalytic ozonation activity and stability for mineralization of six drugs in aqueous solution, including ibuprofen, sulfamethoxazole, phenytoin, diphenhydramine, diclofenac sodium and acyclovir. The characterization studies showed that titanium was incorporated into the framework of γ -Al₂O₃ by Al—O—Ti linkage, locating at tetrahedrally coordinated sites, which increased the Lewis acid sites of γ -Al₂O₃, especially the medium acid sites. The surface atomic oxygen (\equiv Al³⁺—O[•]) and peroxide species (\equiv Ti⁴⁺—O₂[•]) were commonly generated rather than hydroxyl radical from catalytic decomposition of ozone in γ -Ti-Al₂O₃ suspension on the basis of the electron paramagnetic resonance (EPR) and *in situ* Raman measurements. Furthermore, it was verified that the high mineralization of the tested pharmaceuticals came from the surface oxidation of organic acid intermediates by the common role of the surface atomic oxygen and peroxide species.

© 2016 Elsevier B.V. All rights reserved.

1. Introduction

Pharmaceutical compounds (PhACs) occurring in surface and ground waters have been concerned in around the world [1–3]. Some PhACs are very difficult to be removed even by advanced water treatment systems such as adsorption on granular activated carbon or ozonation [4]. Moreover, the chronic exposure of bacteria, algae and other aquatic organisms to trace concentrations of antibiotics raises concerns regarding their ecotoxicological effects, but also their potential to induce bacterial resistance [5–7]. To address these issues, the industry is currently evaluating the need for upgraded wastewater treatment plants to minimize the input of refractory pollutants to an aquatic system.

Heterogeneous catalytic ozonation has gained significant attention as an effective process for the removal of antibiotic functional groups under mild conditions [8]. Metal oxides and supported metals were most widely used in heterogeneous catalytic ozonation.

For catalytic ozonation mechanism, it is generally thought ozone decomposition on the catalyst surface generating hydroxyl radicals and direct ozone oxidation [9,10]. Some researches proposed that ozone decomposition took place on non-dissociated hydroxyl groups of metal oxides [11,12]. Our findings verified that ozone could be chemically adsorbed on the Lewis acid sites of supported and unsupported metal oxides competing with water, and decomposed into reactive oxygen species (ROS) [13–15]. For example, the chemisorbed ozone was decomposed into surface atomic oxygen species at the Lewis acid sites of Al³⁺ while it was converted into surface adsorbed OH_{ads} and O₂^{•-} radicals at the Lewis acid sites of Fe³⁺. Moreover, O₃ was hardly decomposed when it was adsorbed on the hydroxyl groups of weak acid sites of SiO₂ by electrostatic interaction [15,16]. Obviously, the transformation of ozone depends on the surface composition of catalyst, which would greatly affect the transformation of pollutants in water. Hydroxyl radical can unselectively oxidize almost all organics in water due to its high reactivity. However, it is not effective to degrade aliphatic hydrophilic compounds containing carbonyl or carboxylic groups, such as oxalate, because the rate of •OH reacting with these compounds is slower than that one with bicarbonates/carbonates [17]. However, it was found that the oxalate was degraded into CO₂ by

* Corresponding author at: Key Laboratory of Drinking Water Science and Technology, Research Center for Eco-Environmental Sciences, Chinese Academy of Sciences, Beijing 100085, China.

E-mail address: huchun@rcees.ac.cn (C. Hu).

the surface atomic oxygen readily reaction with the surface cerium-oxalate complex over PdO/CeO_2 aqueous suspension [18].

According to the reported work, the gaseous ozone was adsorbed and dissociated into the surface atomic oxygen on strong Lewis acid sites of TiO_2 , Al_2O_3 [16]. Al_2O_3 is widely used as a catalyst in the automotive and petroleum industries due to its low cost, desirable textural properties such as high surface area, mesoporosity, stability, and also its Lewis acid sites [19,20]. Titanium has multivalent and stronger acidity than aluminum, but titanium oxides have relatively low specific surface area [21]. Therefore, the more surface Lewis acid sites can be obtained by the complexes of aluminum and titanium, bringing about more the surface reactive oxygen species in the presence of ozone.

In the present study, $\gamma\text{-Al}_2\text{O}_3$ was prepared as support, titanium was doped into the frame work of mesoporous $\gamma\text{-Al}_2\text{O}_3$ ($\gamma\text{-Ti-Al}_2\text{O}_3$) or loaded on the surface of $\gamma\text{-Al}_2\text{O}_3$ ($\text{TiO}_2/\gamma\text{-Al}_2\text{O}_3$). Six different structures of drugs occurring in the aquatic environment, including ibuprofen (IBU), phenytoin (PHT), diphenhydramine (DP), acyclovir (ACY), sulfamethoxazole (SMX) and diclofenac sodium (DS), were chosen to evaluate the activity and properties of the catalysts. The largest amount of surface Lewis acid sites and highest activity for degradation and mineralization of the selected drugs appeared over $\gamma\text{-Ti-Al}_2\text{O}_3$ with ozone. A surface atomic oxygen and peroxide oxidizing mechanism was proposed.

2. Experimental section

2.1. Catalyst preparation

Mesoporous $\gamma\text{-Ti-Al}_2\text{O}_3$ was prepared by a modified evaporation-induced self-assembly process as described previously for pure $\gamma\text{-Al}_2\text{O}_3$ [22]. Aluminum isopropoxide $[\text{Al}(\text{O}_i\text{Pr})_3]$ was used as Al source and tetrabutyl titanate (TBOT) as Ti source. In a typical procedure, $\text{Al}(\text{O}_i\text{Pr})_3$ (16.8 g), glucose (14.4 g) and a required quantity of TBOT was added in 216 mL deionized water at 35 °C. After stirring for 6 h, the pH of the mixture was adjusted to 5.5 by using a diluted aqueous nitric acid (10 wt.%) solution. The resulting solution was continuously stirred for 24 h and then heated at 100 °C in open air to remove water and all other volatiles. The final solid was calcined at 600 °C for 6 h to obtain $\gamma\text{-Ti-Al}_2\text{O}_3$. Following this procedure, the catalysts containing different Al/Ti ratio ($n_{\text{Al}}/n_{\text{Ti}} = 25, 50, 75, 100$) were prepared. $\gamma\text{-Al}_2\text{O}_3$ was prepared by the above procedure in the absence of TBOT. As references, titanium oxide loaded $\gamma\text{-Al}_2\text{O}_3$ ($\text{TiO}_2/\gamma\text{-Al}_2\text{O}_3$) catalyst with a Ti/Al ratio of 75 was prepared by an impregnation method. In a typical procedure, $\gamma\text{-Al}_2\text{O}_3$ was first dried at 100 °C for 12 h. TBOT was dissolved in deionized water to get a desirable concentration. $\gamma\text{-Al}_2\text{O}_3$ was dispersed into the above titanium solutions under stirring at 35 °C. After stirring for 24 h, the mixture was dried at 100 °C, and then calcined at 600 °C for 6 h to obtain $\text{TiO}_2/\gamma\text{-Al}_2\text{O}_3$.

2.2. Characterization of the catalysts

The powder X-ray diffraction (XRD) of the catalyst was recorded on a Scintag-XDS-2000 diffractometer with $\text{Cu K}\alpha$ radiation ($\lambda = 1.540598 \text{ \AA}$). BET-surface areas were measured by N_2 adsorption using a Micromeritics ASAP2020 automated gas sorption system (USA). The pore size distribution, pore volume, and average pore diameter were determined by the BJH method. The morphologies were obtained using a SU8020 FESEM (Hitachi). The X-ray photoelectron spectroscopy (XPS) data was taken on an AXIS-Ultra instrument (Kratos Analytical, UK) using monochromatic $\text{Al K}\alpha$ radiation (225 W, 15 mA, 15 kV). The infrared spectrum of the dry samples supported on KBr pellets at a fixed amount of

sample (1 wt%), was recorded on a Nicolet 8700 FTIR spectrophotometer (Thermo Fisher Scientific Inc., USA). Infrared spectra of chemisorbed pyridine (Py-FTIR) were obtained on a Bruker Tensor 27 FT-IR spectrometer. The self supported sample wafers were evacuated in a vacuum cell at 100 °C for 2 h prior to pyridine adsorption. After the adsorption of pyridine at room temperature, the samples were out-gassed at 20 °C, 150 °C and 350 °C and their spectra were recorded. The point of zero charge (pH_{pzc}) of the catalysts was measured with a Zetasizer Nano (Malvern, UK) with three average readings.

2.3. Catalytic ozonation procedure

The catalytic degradation experiments of pharmaceuticals were performed in a 1.2 L column reactor at 20 °C. Ozone was produced in situ from pure oxygen by a 3S-A5 laboratory ozone generator (Tonglin Technology, China). In order to allow enough sensitivity for the detection of initial compounds and transformation products, experiments at higher initial concentrations of pharmaceuticals than that ones in real wastewater since due to the small reactor volume no sample preconcentration could be performed. All solutions were prepared with ultrapure water. In a typical procedure, 1 L pharmaceutical around 10 mg L^{-1} aqueous solution and 1.5 g of catalyst powder were mixed in the reactor under continuously magnetically stir. 30 mg L^{-1} of gaseous O_3 oxygen-ozone was continuously bubbled into the reactor through the porous plate of the reactor bottom at a 200 mL min^{-1} flow rate. The same procedures were carried out for the control experiments of ozone alone and sorption without ozone. The residual ozone in the off-gas was trapped by a $\text{Na}_2\text{S}_2\text{O}_3$ solution. Water samples were taken at regular intervals. A 0.1 mol L^{-1} $\text{Na}_2\text{S}_2\text{O}_3$ solution was used to quench the continuous ozonation reaction in the new withdrawn water samples and then water samples were filtered by a 0.45 μm Millipore filter to analyze pharmaceutical and total organic carbon concentrations.

2.4. Analytic methods

All the pharmaceuticals were analyzed by means of an Agilent 1200 series HPLC equipped with a UV detector and a ZORBAX Eclipse XDB-C18 column (4.6 × 150 mm, 5 μm). Total organic carbon (TOC) was measured by a Shimadzu TOC-V_{CPH} analyzer. The released metallic ions from the catalysts in reaction process were determined by ICP-OES on an OPTIMA 2000 (Perkin Elmer Co., U.S.A.). The actual content of aluminum and titanium were also detected by ICP-OES. In a typical procedure, 0.2 g $\gamma\text{-Ti-Al}_2\text{O}_3$ and 30 g $(\text{NH}_4)_2\text{SO}_4$ were put into 70 mL concentrated sulfuric acid under vigorous stirring. The slurry was then refluxed for 24 h. After natural cooling, the supernate was filtered, and the filtrate was diluted and analyzed. The gaseous ozone concentration was measured by an IDEAL-2000 ozone concentration detector (China). The dissolved ozone concentration was determined by the indigo method. Electron Paramagnetic Resonance (EPR) spectra were obtained with a Bruker A300-10/12 EPR spectrometer using BMPO as a spin trap agent at room temperature. In situ Raman spectra of the metal oxides in presence or absence of ozone were taken on a Lab RAM HR Evolution confocal microscopic Raman spectrometer (France) with a 633 nm laser light irradiation. In a typical process, 0.1 g of catalyst powder was added to 2 mL water or ozone aqueous solution (4 mg L^{-1}) and the suspensions were mixed rapidly. Then, 0.2 mL aliquots of sample solutions were immediately collected and placed into the reaction cell, and scanned from 200 to 1200 cm^{-1} at a resolution of 1 cm^{-1} and a duration time of 100 s.

The samples for GC-MS analysis were prepared by the following procedure. The suspension of $\gamma\text{-Ti-Al}_2\text{O}_3$ with different pharmaceuticals (adsorption for 1 h, reaction 5 min and 20 min

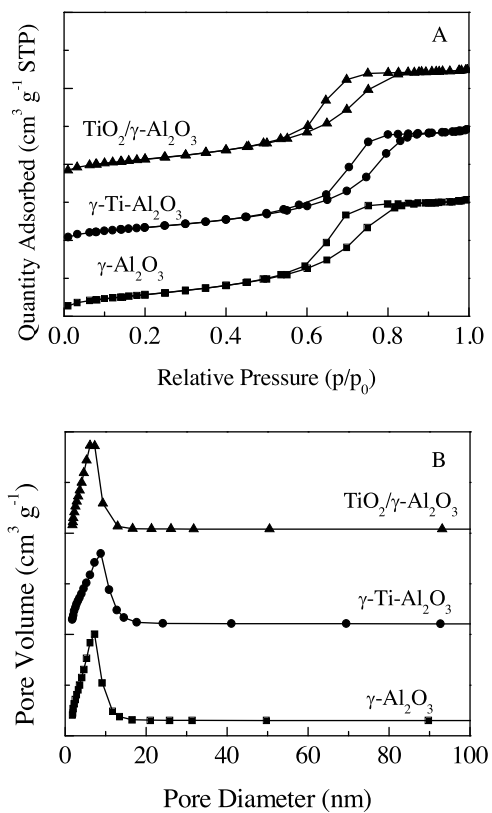


Fig. 1. (A) The N₂ adsorption-desorption isotherms and (B) pore size distribution curves of different catalysts.

Table 1

Surface area, pore diameter and pore volume of different catalysts.

Sample	S _{BET} (m ² g ⁻¹)	Pore diameter (nm)	Pore volume (cm ³ g ⁻¹)
γ-Al ₂ O ₃	248.8	6.13	0.50
TiO ₂ /γ-Al ₂ O ₃	221.9	5.86	0.47
γ-Ti-Al ₂ O ₃	253.1	7.04	0.52

with ozone) was filtered. And the solid particles and the solutions were collected and evaporated by freeze-drying method. Subsequently, the residue was dissolved with 1 mL dichloromethane, and then trimethylsilylated with 0.1 mL of hexamethyldisilazane, and 0.05 mL of chlorotrimethylsilane. The mixture was shaken vigorously for about 60 s and was then allowed to stand for 5 min at room temperature. Precipitate was separated by centrifugation prior to chromatographic analysis. GC-MS analysis was carried out on an Agilent 6890GC/5973MSD with a DB-5 MScapillary column.

3. Results and discussion

3.1. Characterization of the catalysts

The N₂ adsorption-desorption isotherms of the γ-Ti-Al₂O₃, TiO₂/γ-Al₂O₃ catalysts and the γ-Al₂O₃ support are shown in Fig. 1. All the samples provided the IV type isotherm of mesoporous materials with a sharp ramp in the relative pressure range of 0.6–0.8, which was due to the capillary condensation of nitrogen in the pores [23]. The surface area, pore diameter and pore volume increased when a certain amount of titanium was introduced in γ-Al₂O₃ framework (Table 1), which might be due to titanium atoms with larger atomic radius instead of aluminum atom. Oppositely, the relative parameters decreased in the TiO₂/γ-Al₂O₃ catalyst,

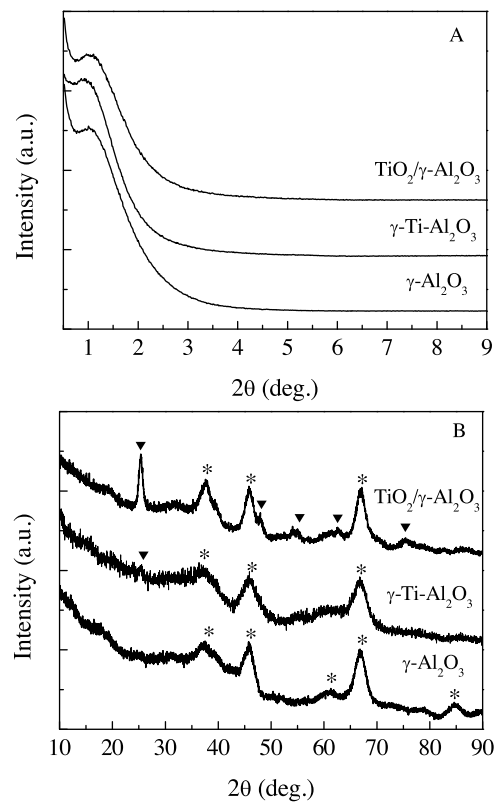


Fig. 2. The low angle (A) and wide angle (B) XRD pattern of different catalysts.

which was possibly due to the coverage of TiO₂ particles blocking the channel of Al₂O₃.

Fig. 2 shows the low angle and wide angle XRD patterns of γ-Al₂O₃, γ-Ti-Al₂O₃ and TiO₂/γ-Al₂O₃. All the samples exhibited a very strong diffraction peak near 1° in the low angle range, which signifies the presence of mesoporous structure [22]. In the wide angle range, typical gamma phase was generated in synthetic Al₂O₃ samples (JCPD no. 00-046-1131), designated by γ-Al₂O₃. For γ-Ti-Al₂O₃ sample, the characteristic peak of γ-Al₂O₃ is retained, and a weak peak appeared at 25.3°, which is assigned to anatase, in γ-Ti-Al₂O₃. While several stronger peaks for anatase (JCPD no. 01-086-1156) appeared in TiO₂/γ-Al₂O₃, which deduced that the titanium species was mainly on the surface of TiO₂/γ-Al₂O₃.

The SEM micrographs of these samples are shown in Fig. 3. It could be clearly seen that the particles of γ-Al₂O₃ samples exhibited spongy porous structure. Both γ-Al₂O₃ and γ-Ti-Al₂O₃ samples exhibited similar surface topography, which was conductive to organic compounds close to catalytic active site. For TiO₂/γ-Al₂O₃ catalyst, large particles of titanium oxide were found on the outer surface of γ-Al₂O₃ indicating that the titanium oxide particles were not well-dispersed.

Fig. 4 shows the Al 2p, Ti 2p and O 1s XPS spectra of different samples. Since the Ti 2p 3/2 XPS spectra exhibit two binding energies (BEs) of Ti⁴⁺ at 458.9 eV and Ti³⁺ at 457.9 eV [24], in the TiO₂/γ-Al₂O₃ catalyst, titanium oxide mainly existed in Ti³⁺ on the surface of the material, while in the fresh and the used γ-Ti-Al₂O₃, titanium existed in the form of Ti⁴⁺. Both γ-Al₂O₃ and TiO₂/γ-Al₂O₃ have similar Al 2p XPS spectra, binding energy of Al³⁺ at 74.3 eV, assigned to Al—O—Al [25]. In γ-Ti-Al₂O₃ sample, however, the Al 2p XPS spectra exhibit two BEs of Al³⁺ at 74.3 and 75.3 eV, assigned to Al—O—Al and Al—O—Ti respectively [26,27]. In addition, the peak at 1128.3 cm⁻¹ appeared at the FTIR spectra of γ-Ti-Al₂O₃, assigned to the surface Al—O—Ti groups (Fig. 5) [28], verifying titanium in the form of Al—O—Ti in the framework of γ-Ti-Al₂O₃. The O 1s XPS

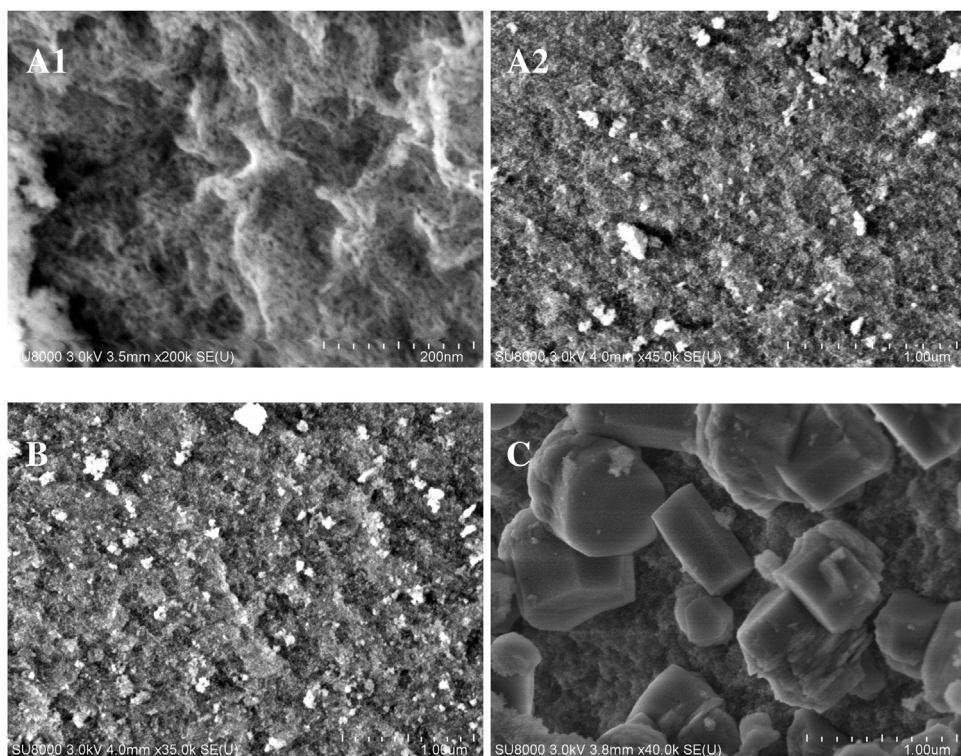


Fig. 3. SEM images of γ -Al₂O₃ (A1 and A2), γ -Ti-Al₂O₃ (B) and TiO₂/ γ -Al₂O₃ (C).

Table 2

Al and Ti content in the whole particle and the surface phase of different catalysts.

Sample	$n_{\text{Al}}/n_{\text{Ti}}$	Element in the bulk (wt%)		Element on the surface (wt%)	
		Al	Ti	Al	Ti
γ -Ti-Al ₂ O ₃	75	51.84	1.31	49.77	1.29
TiO ₂ / γ -Al ₂ O ₃	75	52.45	1.36	45.38	8.03

spectra of γ -Al₂O₃ and TiO₂/ γ -Al₂O₃ exhibited common peak at 531.4 eV, which is usually assigned to the lattice oxygen. In γ -Ti-Al₂O₃ sample, besides the peak at 531.4 eV, the peak at 532.3 eV appeared, which is attributed to the chemical adsorption of oxygen at oxygen vacancy [29,30]. Surface chemisorbed oxygen (O) has been reported to be more active than lattice oxygen due to its higher mobility and plays an important role in oxidation reactions.

In Table 2, the Ti concentration in the whole particle and the surface phase of γ -Ti-Al₂O₃ is almost the same, indicating titanium is well dispersed in the material. While the surface Ti concentration was 8.03 wt% compare with 1.36 wt% in bulk for TiO₂/ γ -Al₂O₃, indicating that most of Ti was supported on the surface of TiO₂/ γ -Al₂O₃.

The nature and strength of the surface acid sites on γ -Al₂O₃, γ -Ti-Al₂O₃ and TiO₂/ γ -Al₂O₃ were determined by FTIR of adsorbed pyridine. Fig. 6 presents the evolution of the relevant pyridine vibrational bands as a function of the annealing temperatures (20 °C, 150 °C and 350 °C). These vibrational modes within 1700–1200 cm⁻¹ correspond to various pyridine ring stretching modes ν (C–N) and ν (C–C) [31]. At 20 °C, all oxide materials exhibited the pyridine adsorption at 1221, 1448, 1492, 1578, 1595 and 1614 cm⁻¹ (Fig. 6A), besides this, a peak at 1308 cm⁻¹ appeared in γ -Ti-Al₂O₃. Among of them, the observed IR bands at 1221, 1308, 1448, 1492 and 1614 cm⁻¹ were attributed to the formation of pyridine species coordinated to the surface Lewis acid sites [32]. The band at around 1595 cm⁻¹ completely disappeared at 150 °C (Fig. 6B), which is assigned to the presence of a weakly

Table 3

Amount of Lewis acid sites of different catalysts determined by Py-FTIR ($\mu\text{mol g}^{-1}$).

Sample	Total acid	Medium acid	Strong acid
γ -Al ₂ O ₃	540.1	197.4	61.1
TiO ₂ / γ -Al ₂ O ₃	653.8	222.9	85.4
γ -Ti-Al ₂ O ₃	947.3	733.1	202.2

interacting pyridine species, which is coordinated to the surface via hydrogen bonding. While the band at 1578 cm⁻¹ almost completely disappeared at temperatures 350 °C (Fig. 6C), which was attributed to medium-strength Lewis acid sites. With increasing annealing temperatures, the other bands shifted to higher frequencies, suggesting that this IR feature was associated with the pyridine adsorption on more strong Lewis acid sites. The additional visible peak at 1308 cm⁻¹ appeared in γ -Ti-Al₂O₃ was associated to the Ti⁴⁺ exists in the framework with a tetrahedral coordination [31,33]. An attempt has also been made to quantitatively estimate the number of Lewis acid sites for the three catalysts using pyridine adsorption followed by degassing at 20, 150 and 350 °C, corresponding to the total, medium and strong acid sites (Table 3) [34]. γ -Ti-Al₂O₃ can greatly increase the Lewis acid sites of Al₂O₃ than TiO₂/ γ -Al₂O₃ sample. Besides, the quantity ratio of total acid, medium acid and strong acid is about 3 in γ -Al₂O₃ and TiO₂/ γ -Al₂O₃ catalysts. However, a larger percentage of medium acid appeared in γ -Ti-Al₂O₃ samples. These results suggested that the doped titanium into the framework position of γ -Al₂O₃ altered the surface acidity of the alumina surface, especially increasing the medium acid sites.

3.2. Catalytic activity for the degradation of selected pharmaceuticals

Fig. 7 exhibited the influence of titanium doping content (Al/Ti) on catalytic activity of γ -Ti-Al₂O₃ for ozonation of ibuprofen (IBU). The catalyst with Al/Ti ratio of 75 exhibited the highest activity for

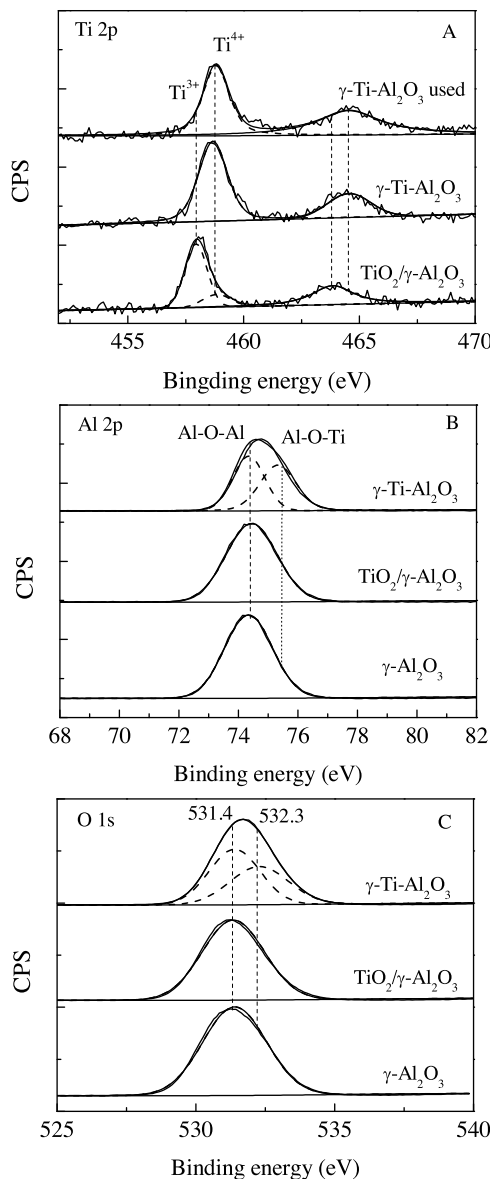


Fig. 4. Ti 2p (A), Al 2p (B) and O 1s (C) XPS spectra of γ - Al_2O_3 , TiO_2/γ - Al_2O_3 , γ - $\text{Ti-Al}_2\text{O}_3$ and γ - $\text{Ti-Al}_2\text{O}_3$ used.

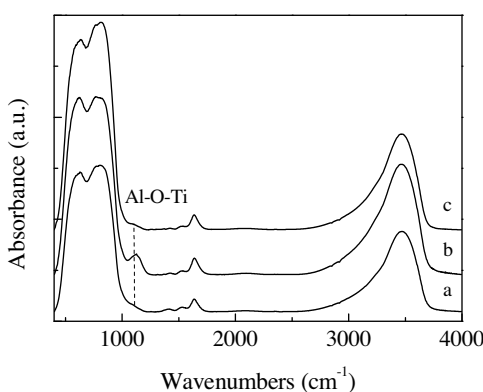


Fig. 5. FTIR spectra of (a) γ - Al_2O_3 , (b) γ - $\text{Ti-Al}_2\text{O}_3$ and (c) TiO_2/γ - Al_2O_3 .

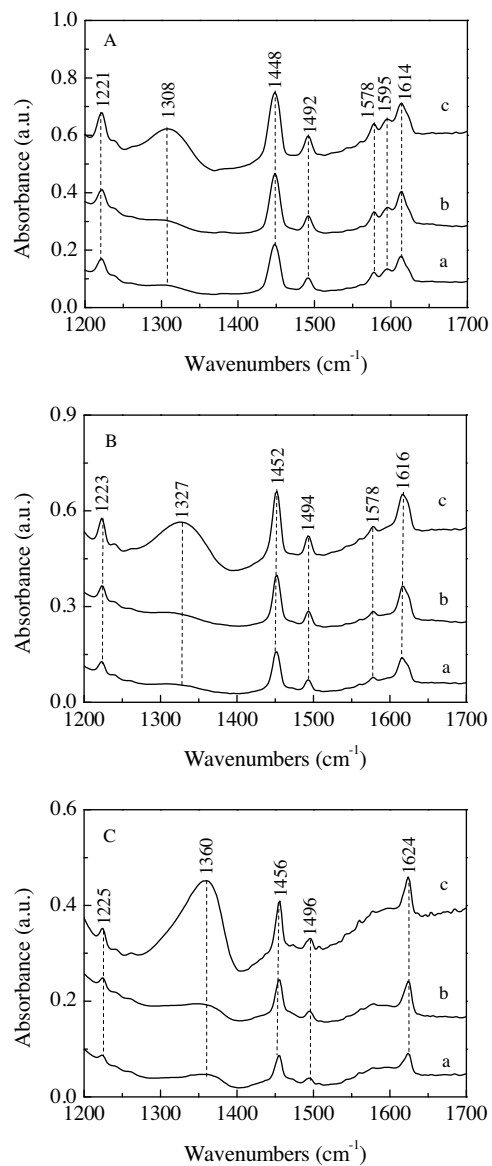


Fig. 6. Py-FTIR spectra of (a) γ - Al_2O_3 , (b) TiO_2/γ - Al_2O_3 and (c) γ - $\text{Ti-Al}_2\text{O}_3$ after degassing at (A) 20 °C, (B) 150 °C, (C) 350 °C.

catalytic ozonation of IBU, and was used for all the experiments unless otherwise specified. Fig. 8 shows that the performance of different catalyst evaluation by ibuprofen (IBU). The presence of catalyst was advantageous for IBU degradation compared with ozonation alone, and γ - $\text{Ti-Al}_2\text{O}_3$ had the highest catalytic activity. Though IBU was completely degraded in all processes at 20 min reaction time, a maximum of 98% TOC removal was obtained at 60 min oxidation time with γ - $\text{Ti-Al}_2\text{O}_3$, while about 80%, 62%, 32% and 26% of TOC were removed at the same time in TiO_2/γ - Al_2O_3 , γ - Al_2O_3 , TiO_2 and ozonation alone processes, respectively. Because only 5% TOC removal by γ - $\text{Ti-Al}_2\text{O}_3$ adsorption (Fig. S1). It indicated that there was a significant synergistic effect (between adsorption and ozonation alone in γ - $\text{Ti-Al}_2\text{O}_3/\text{O}_3$ process). Furthermore, the catalytic activity of different catalysts is consistent with the amount of surface Lewis acid site. γ - $\text{Ti-Al}_2\text{O}_3$ had the greatest amount of Lewis acid sites, resulting the highest activity. Furthermore, the catalytic ozonation and ozonation of IBU was carried out in the ultrapure water with HA or in the real water (Fig. S2), and the water quality parameters was shown in Table S1. Obviously, the degradation of IBU was enhanced under both conditions with catalytic

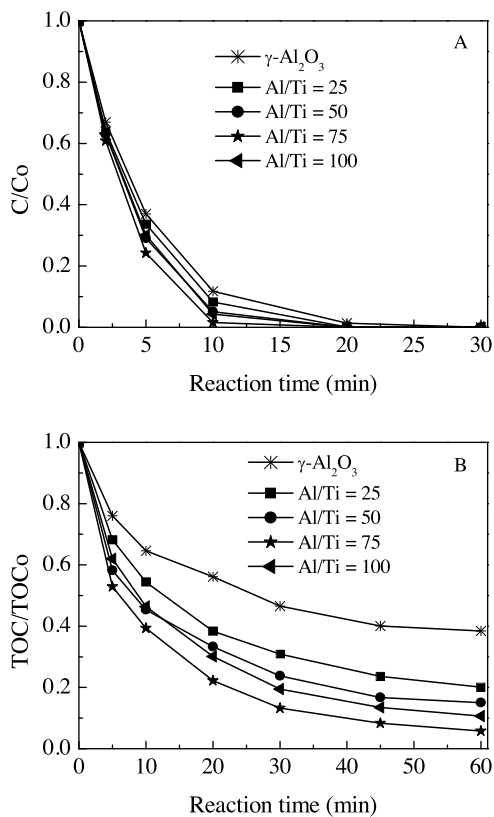


Fig. 7. Effect of titanium doping amount of γ -Ti-Al₂O₃ on IBU (A) and TOC (B) removal. (Initial pH = 7.0, initial IBU concentration = 10 mg L⁻¹, catalyst concentration = 1.5 g L⁻¹).

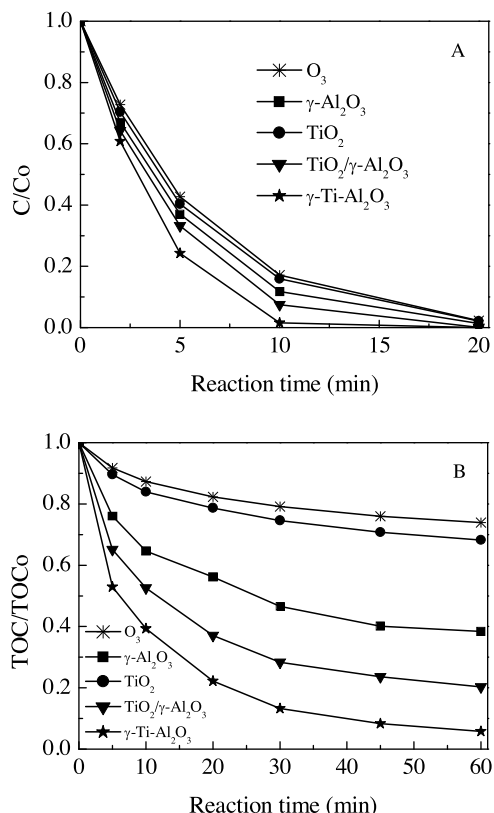


Fig. 8. Comparison IBU and TOC removal by different processes. (Initial pH = 7.0, initial IBU concentration = 10 mg L⁻¹, catalyst concentration (if use) = 1.5 g L⁻¹).

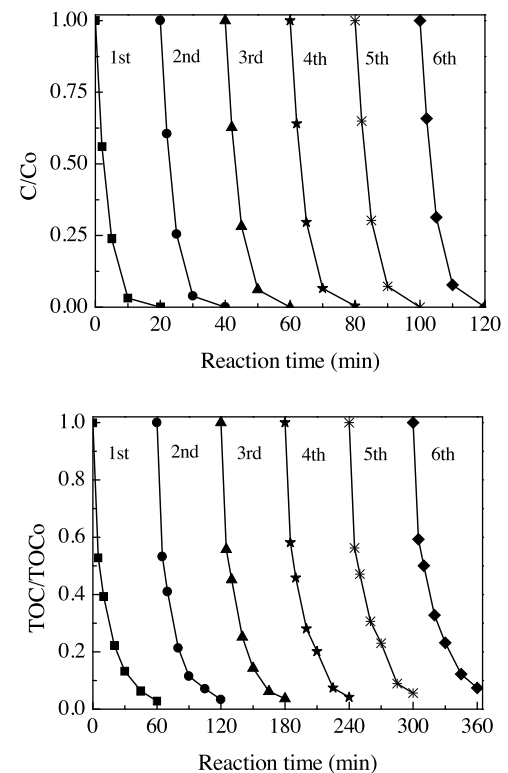


Fig. 9. Stability of γ -Ti-Al₂O₃ in catalytic ozonation process. (Initial pH = 7.0, initial IBU concentration = 10 mg L⁻¹, catalyst concentration = 1.5 g L⁻¹).

ozonation or ozonation process. Compared to ultrapure water, the TOC removal was also improved in the real water (Fig. S2B), while the TOC removal rate decreased slightly in the presence of HA with ultrapure water. The results indicated that IBU and dissolved organics (DOC) competed for ROS in catalytic ozonation, which depended on their concentration in water. The stability of γ -Ti-Al₂O₃ was evaluated by repeated degradation testing use (Fig. 9). The activity of γ -Ti-Al₂O₃ did not markedly decrease after six successive cycles, and there was not any titanium and aluminum leaching in all the reuse cycle. The results illustrated that γ -Ti-Al₂O₃ catalyst was provided with a high catalytic activity and chemical stability by titanium incorporated into the framework of γ -Al₂O₃.

The γ -Ti-Al₂O₃ catalytic ozonation was also performed for other pharmaceuticals, including sulfamethoxazole (SMX), phenytoin (PHT), diphenhydramine (DP), diclofenac sodium (DS) and acyclovir (ACY), which were selected according to their structure and adsorption on γ -Ti-Al₂O₃. The molecular structures are shown in Fig. S3. The comparison of ozonation alone and γ -Ti-Al₂O₃ catalytic ozonation of the five different pharmaceuticals was shown in Fig. 10. The TOC removal efficiency was only 36% (DP), 28% (SMX), 34% (PHT), 13% (ACY) and 38% (DS) in ozonation process at 60 min reaction time. While TOC removal efficiency was considerably improved to 92% (DP), 92% (SMX), 96% (PHT), 65% (ACY) and 99% (DS) in catalytic ozonation process at the same time. The adsorption of DP, SMX, PHT, ACY and DS by γ -Ti-Al₂O₃ was about 3%, 8%, 4%, 0.1% and 6% in equilibrium (Fig. S1), respectively. ACY could hardly adsorb on the surface of the γ -Ti-Al₂O₃, a lowest mineralization rate appeared in catalytic ozonation. This result shows that the adsorption of the drugs on the surface of γ -Ti-Al₂O₃ is beneficial to the mineralization. In addition, compared with the ozonation processes, the selected drugs were almost completely mineralized except ACY in the catalytic ozonation processes. These results illustrated that γ -Ti-Al₂O₃ was a promising catalyst for ozonation of pharmaceuticals in aqueous solution.

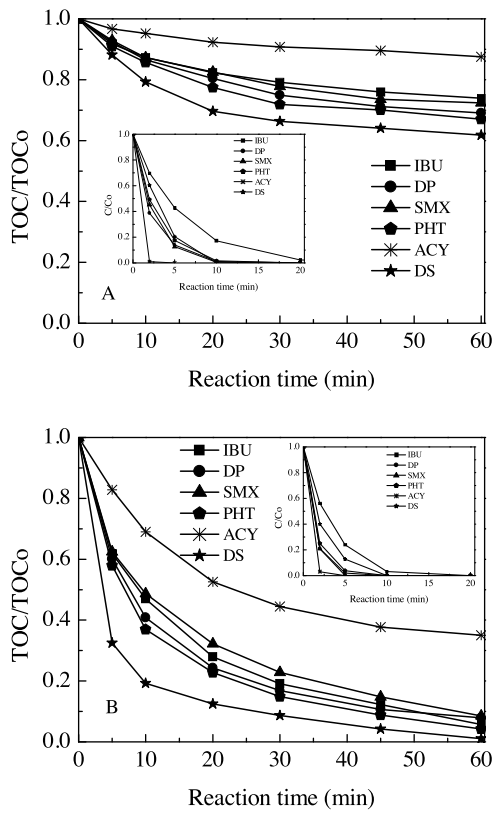


Fig. 10. Comparison of ozonation alone (A) and γ -Ti-Al₂O₃ catalytic ozonation (B) of six drugs. (Initial pH = 7.0, initial drug concentration = 10 mg L⁻¹, catalyst concentration = 1.5 g L⁻¹).

3.3. The surface reaction mechanism

According to the previous investigation, ozone could be adsorbed and decomposed into reactive oxygen species on the Lewis acid sites of catalysts competing with water [13,15]. EPR spin-trap technique with BMPO was used to detect the radicals in different catalysts suspensions with ozone (Fig. 11). The O₂^{•-} and OH signals were increased according to the following order of γ -Al₂O₃, TiO₂/ γ -Al₂O₃ and γ -Ti-Al₂O₃. However, their peak intensities were lower than those ones in ozone alone aqueous solution, indicating that the adsorbed ozone on the surface was hardly decomposed into O₂^{•-} and OH radicals. *tert*-Butanol (TBA) is a strong radical scavenger, and cannot be adsorbed on the surface of metal oxides for its physical-chemical property [35]. Therefore, TBA predominantly scavenged free OH in solution in γ -Ti-Al₂O₃ suspensions with ozone. Its addition caused less suppression of IBU degradation in catalytic ozonation than ozone alone at pH 7 (Fig. 12), suggesting that the OH radicals in solution were not dominant reactive oxygen species in γ -Ti-Al₂O₃ catalytic ozonation. The results suggested that the surface reactive oxygen species might play important role for the degradation and mineralization of IBU in the catalytic ozonation. In situ Raman spectroscopy was used to characterize intermediate oxygen species formed on γ -Al₂O₃, TiO₂/ γ -Al₂O₃ and γ -Ti-Al₂O₃ with ozone aqueous solution (Fig. 13). In γ -Al₂O₃ dispersion, a new band appeared at 945 cm⁻¹ with ozone aqueous solution, assigned to surface atomic oxygen species (\equiv Al—*O) [36,37]. In TiO₂/ γ -Al₂O₃ suspension with ozone, a characterized peak at 892 cm⁻¹ assigned to surface peroxide species (\equiv Ti—*O₂) [38,39], whereas two new peaks appeared at 880 and 930 cm⁻¹ in γ -Ti-Al₂O₃ suspension with ozone, which are still characteristic features of surface peroxide (*O₂) and surface atomic oxygen species (*O), respectively. However, the peak wavenumbers

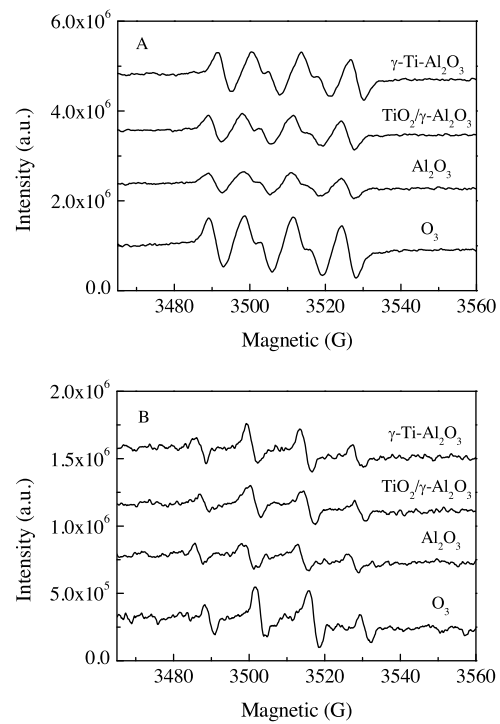


Fig. 11. BMPO spin-trapping EPR spectra recorded in methanol dispersion for BMPO—HO₂[•]/O₂^{•-} (A) and aqueous dispersion for BMPO[•]-OH (B) with ozone. (Initial pH = 7.0, catalyst concentration (if use) = 2 g L⁻¹, initial BMPO concentration = 25 mM).

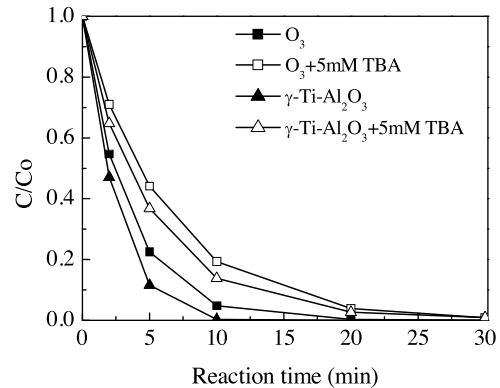


Fig. 12. Effect of TBA on ozonation and catalytic ozonation of IBU. (Initial pH = 7.0, initial IBU concentration = 10 mg L⁻¹, catalyst concentration (if use) = 1.5 g L⁻¹).

were lower than the values observed for γ -Al₂O₃ and TiO₂/ γ -Al₂O₃. This can be attributed to the generation of Al—O—Ti linkage by doping titanium into the framework that changes the bind strength between aluminum and these surface oxygen-containing species. The high oxidation potential of surface atomic oxygen (2.43 V in water) and peroxide species (1.35 V in protonated form) were the reactive oxygen species in γ -Ti-Al₂O₃ catalytic ozonation process. The results indicated that the high mineralization of the tested pharmaceuticals came from the common role of surface atomic oxygen and peroxide species. Therefore, γ -Ti-Al₂O₃ had certain adsorption to IBU, DP, SMX, PHT and DS, resulting in their high mineralization rate, while γ -Ti-Al₂O₃ hardly adsorbed ACY, leading its low mineralization rate. Furthermore, the effect of pH on ozonation and γ -Ti-Al₂O₃ catalytic ozonation of IBU was investigated (Fig. 14). In ozonation process, IBU and TOC removal increased with initial pH from 3.0 to 9.0. At 60 min oxidation time, the maximum TOC removal (40%) was achieved at pH 9.0 only 32%, 15% and 10%

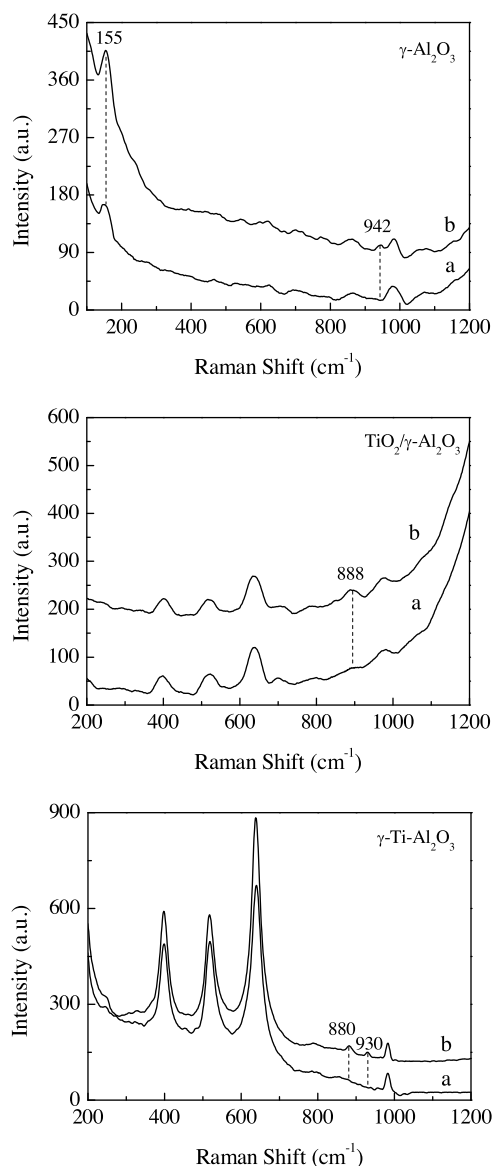


Fig. 13. Raman spectra of γ -Al₂O₃, TiO₂/ γ -Al₂O₃ and γ -Ti-Al₂O₃ aqueous dispersions without (a) and with (b) ozone. (Catalyst concentration = 33.3 g L⁻¹, ozone concentration in water = 4.23 mg L⁻¹, initial pH = 7.0).

at pH 7.0, 5.0 and 3.0, respectively. This is because OH^- is mainly hydroxyl radical initiator in ozonation alone [19]. In γ -Ti-Al₂O₃ catalytic ozonation process, the IBU degradation rate increased with increasing initial pH, while TOC removal rate was greatly increased compared with ozonation alone, and the TOC removal increased with increasing initial pH from 3.0 to 7.0, but at pH 9, TOC removal rate greatly decreased. The pH_{pzc} of γ -Ti-Al₂O₃ was 7.3, so the surface of the γ -Ti-Al₂O₃ was positively charged in the range of pH < 7, while the surface exhibited negative zeta-potential at pH 9. So the ionized IBU can be adsorbed onto the surface of γ -Ti-Al₂O₃ by electrostatic attraction at pH < 7, while IBU and organic acid intermediates hardly had any adsorption on the negative charged surface at pH 9 due to repulsive force, where the degradation of these compounds was mainly due to the oxidation of ozone and hydroxyl radical in aqueous solution. The results also indicated that organic acid byproducts from IBU degradation mainly occurred on the surface of γ -Ti-Al₂O₃.

The common role of surface atomic oxygen and peroxide species facilitates the mineralization of organic acids by sur-

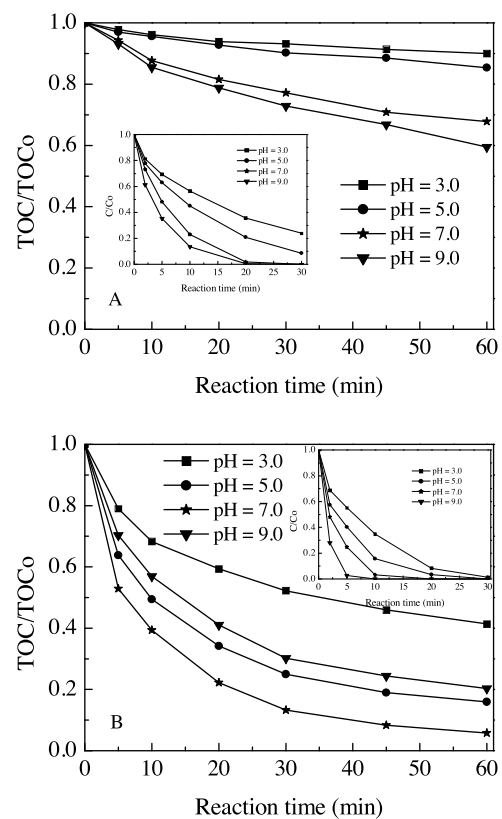


Fig. 14. Effect of initial pH on IBU and TOC removal in ozonation alone (A) and γ -Ti-Al₂O₃ catalytic ozonation (B) process. (Initial IBU concentration = 10 mg L⁻¹, catalyst concentration = 1.5 g L⁻¹).

face reactions, the analysis of the intermediate products of drugs degradation by γ -Ti-Al₂O₃ catalytic ozonation further proved this point. The main products in the aqueous solution and on the surface of γ -Ti-Al₂O₃ were collected and analyzed at reaction time of 5 and 20 min (Table S2). During the ibuprofen degradation, 5 intermediates produced at 5 min, including 2-oxopropanoic acid, 2-hydroxy-3-methylbutanoic acid, propane-1,2,3-triol, 4-isobutylphenol and 4-isobutylbenzoic acid. Meanwhile, 6 organic acids were detected on the surface of the catalyst, such as oxalic acid, malonic acid, 3-methyl-2-oxobutanoic acid, maleic acid, 4-hydroxybenzoic acid and 3,4,5-trihydroxybenzoic acid. While at the reaction time of 20 min, only some aliphatic acids in the solution, such as oxalic acid, 2-methylpropan-1-ol, 2-hydroxyacetic acid and propane-1,2,3-triol. Moreover, on the surface of the catalyst, the larger molecular weight organic acids are detected, such as 2-hydroxy-3-methylbutanoic acid, maleic acid, and 2-(3,4-dihydroxyphenyl)-2-hydroxyacetic acid and 2,3,4,5,6-pentahydroxyhexanone. The results showed that the mineralization of ibuprofen and its degradation products organic acids was mainly occur on the surface of γ -Ti-Al₂O₃, and the mineralization process was shown to proceed with aromatic ring fracture to organic acid, to carbon dioxide and water. Similar processes were observed in the degradation of PHT, DP, DS and SMX. In the contrast, in the degradation process of ACY, most of intermediates were detected in solution, while little compounds appeared on the surface of γ -Ti-Al₂O₃. For example, at the reaction time of 5 min in solution, 5 intermediates appeared, including ethane-1,2-diol, hydroxycarbamic acid, (E)-2-(amino (hydroxy) methyleneamino) acetic acid, 2- amino-1H-purin-6(9H)-one and 5-hydroxy-1-((2-hydroxyethoxy)methyl)-1H-imidazole-4-carboxamide. On the surface, only 2 compounds 2-amino-1H-purin-6(9H)-one and hydroxycarbamic acid were detected. At the reaction time

of 20 min, in solution, 7 compounds were detected, hydroxycarbamic acid, (*E*)-2-(amino(hydroxy)methyleneamino) acetic acid and 2-amino-1H-purin-6(9H)-one remained, 2-aminoacetic acid, 2,3,3-trihydroxyacrylic acid, 2-hydroxy-1H-purin-6(9H)-one and 5,6-diaminopyrimidine-2,4-diol appeared. On the surface of γ -Ti-Al₂O₃, only 2,3,3-trihydroxyacrylic acid and 5,6-diaminopyrimidine-2,4-diol appeared. The results showed that ACY and its degradation products were hardly adsorbed on γ -Ti-Al₂O₃ surface, degradation reaction predominantly occurred in solution, leading lower mineralization rate.

4. Conclusions

Mesoporous γ -Ti-Al₂O₃ was successfully prepared and showed excellent catalytic ozonation activity and stability for mineralization of ibuprofen, sulfamethoxazole, phenytoin, diphenhydramine, diclofenac sodium and acyclovir at the higher concentration (10 mg L⁻¹) in ultrapure water. Titanium was incorporated into the framework of γ -Al₂O₃, locating at tetrahedrally coordinated sites. The amounts of Lewis acid was greatly increased in γ -Ti-Al₂O₃ catalyst, especially the medium acid sites, which was attributed to the formation of Al—O—Ti linkage in the framework of γ -Ti-Al₂O₃. EPR and *in situ* Raman studies confirmed that the surface atomic oxygen (\equiv Al³⁺—*O) and peroxide species (\equiv Ti⁴⁺—*O₂) were commonly generated rather than hydroxyl radical from catalytic decomposition of ozone in γ -Ti-Al₂O₃ suspension. The high mineralization of the tested PhACs at higher concentration came from the surface oxidization of organic acid intermediates by the common role of the surface atomic oxygen and peroxide species. For real water, catalytic ozonation of the tested PhACs probably exhibit different status from DOC competition for ROS due to their much lower concentration than DOC.

Acknowledgments

This work was supported by National Key Research and Development Plan (2016YFA0203200) and the National Natural Science Foundation of China (Grant Nos. 51538013 and 51138009).

Appendix A. Supplementary data

Supplementary data associated with this article can be found, in the online version, at <http://dx.doi.org/10.1016/j.apcatb.2016.09.019>.

References

[1] M.J. Benotti, R.A. Trenholm, B.J. Vanderford, J.C. Holady, B.D. Stanford, S.A. Snyder, Environ. Sci. Technol. 43 (2009) 597–603.

[2] Y. Lee, D. Gerrity, M. Lee, A.E. Bogaert, E. Salhi, S. Gamage, R.A. Trenholm, E.C. Wert, S.A. Snyder, U. von Gunten, Environ. Sci. Technol. 47 (2013) 5872–5881.

[3] T. Heberer, Toxicol. Lett. 131 (1–2) (2002) 5–17.

[4] O.A. Jones, J.N. Lester, N. Voulvouli, Trends Biotechnol. 23 (4) (2005) 163–167.

[5] F. Bonvin, J. Omlin, R. Rutler, W.B. Schweizer, P.J. Alaimo, T.J. Strathmann, K. McNeill, T. Kohn, Environ. Sci. Technol. 47 (2013) 6746–6755.

[6] J.-M. Brozinski, M. Lahti, A. Meierjohann, A. Oikari, L. Kronberg, Environ. Sci. Technol. 47 (2012) 342–348.

[7] C. Prasse, M. Wagner, R. Schulz, T.A. Ternes, Environ. Sci. Technol. 46 (2012) 2169–2178.

[8] B. Legube, N. Karpel Vel Leitner, Catal. Today 53 (1999) 61–72.

[9] B. Kasprzyk-Hordern, M. Ziolk, J. Nawrocki, Appl. Catal. B 46 (2003) 639–669.

[10] J. Nawrocki, B. Kasprzyk-Hordern, Appl. Catal. B 99 (2010) 27–42.

[11] F. Qi, Z. Chen, B. Xu, J. Shen, J. Ma, C. Joll, A. Heitz, Appl. Catal. B 84 (2008) 684–690.

[12] T. Zhang, J. Ma, J. Mol. Catal. A: Chem. 279 (2008) 82–89.

[13] A. Lv, C. Hu, Y. Nie, J. Qu, Appl. Catal. B 100 (2010) 62–67.

[14] L. Yang, C. Hu, Y. Nie, J. Qu, Environ. Sci. Technol. 43 (2009) 2525–2529.

[15] J. Bing, C. Hu, Y. Nie, M. Yang, J. Qu, Environ. Sci. Technol. 49 (2015) 1690–1697.

[16] K.M. Bulanik, J.C. Lavalley, A.A. Tsyganenko, Colloids Surf. A 101 (1995) 153–158.

[17] U. von Gunten, Water Res. 37 (2003) 1443–1467.

[18] T. Zhang, W. Li, J.-P. Croué, Environ. Sci. Technol. 45 (2011) 9339–9346.

[19] S. Roy, G. Mpourmpakis, D.-Y. Hong, D.G. Vlachos, A. Bhan, R.J. Gorte, ACS Catal. 2 (2012) 1846–1853.

[20] M. Trueba, S.P. Trasatti, Eur. J. Inorg. Chem. 2005 (2005) 3393–3403.

[21] F. Jiang, L. Zeng, S. Li, G. Liu, S. Wang, J. Gong, ACS Catal. 5 (2015) 438–447.

[22] B. Xu, T. Xiao, Z. Yan, X. Sun, J. Sloan, S.L. González-Cortés, F. Alshahrani, M.L.H. Green, Microporous Mesoporous Mater. 91 (2006) 293–295.

[23] Y. Bang, S. Park, S.J. Han, J. Yoo, J.H. Song, J.H. Choi, K.H. Kang, I.K. Song, Appl. Catal. B 180 (2016) 179–188.

[24] H. Jeon, J. Park, W. Jang, H. Kim, S. Ahn, K.-J. Jeon, H. Seo, H. Jeon, Carbon 75 (2014) 209–216.

[25] C.M.A. Parlett, L.J. Durndell, A. Machado, G. Cibin, D.W. Bruce, N.S. Hondon, K. Wilson, A.F. Lee, Catal. Today 229 (2014) 46–55.

[26] L.H. Kim, K. Kim, S. Park, Y.J. Jeong, H. Kim, D.S. Chung, S.H. Kim, C.E. Park, ACS Appl. Mater. Interfaces 6 (2014) 6731–6738.

[27] D. Zhao, C. Chen, Y. Wang, W. Ma, J. Zhao, T. Rajh, L. Zang, Environ. Sci. Technol. 42 (2008) 308–314.

[28] V. Gun'ko, V. Zarko, V. Turov, R. Leboda, E. Chibowski, E. Pakhlov, E. Goncharuk, M. Marciniak, E. Voronin, A. Chuiko, J. Colloid Interface Sci. 220 (1999) 302–323.

[29] S. Karthikeyan, D.D. Dionysiou, A.F. Lee, S. Suvitha, P. Maharaja, K. Wilson, G. Sekaran, Catal. Sci. Technol. 6 (2016) 530–544.

[30] W. Zhao, Y. Tang, Y. Wan, L. Li, S. Yao, X. Li, J. Gu, Y. Li, J. Shi, J. Hazard. Mater. 278 (2014) 350–359.

[31] S.M. Andonova, G.S. Şentürk, E. Kayhan, E. Ozensoy, J. Phys. Chem. C 113 (2009) 11014–11026.

[32] K. Morishige, S. Kittaka, S. Katsuragi, T. Morimoto, J. Chem. Soc. J. Chem. Soc. Faraday Trans. I 78 (1982) 2947–2957.

[33] J. Li, Y. Zhu, R. Ke, J. Hao, Appl. Catal. B 80 (2008) 202–213.

[34] C.A. Emeis, J. Catal. 141 (1993) 347–354.

[35] T. Turan-Ertas, M.D. Gurol, Chemosphere 47 (2002) 293–301.

[36] M. Che, A.J. Tench, in: H.P.D.D. Eley, B.W. Paul (Eds.), *Advances in Catalysis*, Academic Press, 1983, pp. 1–148.

[37] W. Li, G.V. Gibbs, S.T. Oyama, J. Am. Chem. Soc. 120 (1998) 9041–9046.

[38] R. Radhakrishnan, S.T. Oyama, J. Catal. 199 (2001) 282–290.

[39] R. Radhakrishnan, S.T. Oyama, J.G. Chen, K. Asakura, J. Phys. Chem. B 105 (2001) 4245–4253.